Atomic Force Microscopy Studies in Various Environments

Application Note

Sergei Magonov
Agilent Technologies

Abstract

Atomic force microscopy imaging of organic and polymer samples with Agilent 5500 microscope in humid air and vapors of solvents (methanol, toluene, benzene, tetrahydrofuran) is presented. The observed vapor-induced structural transformations and swelling of the samples improves characterization of these objects at the small scales.

Introduction

Comprehensive characterization of surface structures with atomic force microscopy (AFM) is one of the important areas of modern science and technology. The essence of this technique is the use of a miniature probe, which consists of a cantilever with a tip at its free end, for a detection of different tip-sample forces. The optical level method, in which the cantilever deflection or oscillation in a response to the tip apex interacting with a sample is magnified on a photodetector, provides unique sensitivity. This sensitivity combined with the high-precision 3D translation of the probe over the sample surface makes the atomic force microscope the unique tool for visualization of atomic and molecular-scale structures. The applications of AFM are not limited to high-resolution and low-force profilometry. The probe sensitivity to mechanical and electromagnetic tip-sample interactions allows using it for local examination of various materials properties and related compositional mapping. In addition, AFM can be applied in a broad range of environments (UHV, air, liquid, gases, etc). This is the unique feature of the microscopic method that makes it a necessary tool in research laboratories. Naturally, imaging under liquid has attracted a major interest because of biological studies and, despite some difficulties related to the control of oscillatory AFM techniques in viscous media, these applications are well recognized. On other side, the use of AFM in ultra high vacuum (UHV) is also well-established with its own specifics. In UHV the quality factor of the probe is extremely high and this makes frequency modulation mode practically exclusive for the applications. Such studies are addressing fundamental issues of surface science and catalysis with the experiments performed on clean crystalline samples at the atomic-scale. A high-cost of UHV equipment and labor-intensive measurements does not allow this field to become expansive. There is another area of AFM applications i.e. the studies in different gas environments that is not yet in the focus of many researchers. A potential of observing new phenomena in the environmental experiments is very high because AFM is practically the only microscopic technique that provides an access to materials and their changes caused by the environment.

Agilent Technologies

A short review of AFM measurements in various gas environments is the subject of this Application Note. The studies were performed on different organic and polymer samples in an environmental chamber of the Agilent 5500 scanning probe microscope, Figure 1. A sample plate is at the top of the chamber, which is made of glass and has several fittings limiting an exchange with the laboratory air. Injection of a small volume (1-3 ml) of water or organic solvents to the bottom of the chamber followed by its evaporation will change the sample environment making it humid or filled with organic vapors. The humidity level is judged by a humidity meter inserted into the chamber and drying can be assisted by purging inert gases (such as nitrogen or argon) through four ports. Methanol, toluene, benzene and tetrahydrofuran were applied in our studies, some of them continued for many hours, and these solvents did not cause any deterioration of the microscope.

Figure 1. An environmental chamber of Agilent 5500 scanning probe microscope. The humidity meter shows 92% RH environment.

spirals were preserved on the surface basically for unlimited time. These observations can be rationally explained by a sublimation of self-assemblies formed of shorter $F_{12}H_8$ molecules. The self-assemblies are constructed of fluoroalkane molecules with chains oriented in the vertical direction with the fluorinated parts facing air [2]. This will explain the height difference of the $F_{12}H_{20}$ and $F_{12}H_8$ self-assemblies. Their identical surface potential is related to strength and orientation of molecular dipole at the $-CH_2-CF_2-$ central junction [3]. Weak intermolecular interactions between the fluoroalkanes molecules lead to the sublimation of their shorter homologs at ambient conditions.

Specific features of using different substrates such as gold and graphite in ambient conditions studies should be considered by AFM practitioners. Our earlier surface potential studies revealed that Au(111) and graphite substrates are contaminated in air: the first one – fast, the second slowly, within the hours. In air, graphite and similar substrates, e.g. MoS_2, can be covered by molecular layers of volatile compounds. For example, a presence of dodecanol vapor near these substrates might induce a formation of stripped molecular patterns on their surface. The phase images of such patterns

AFM Studies in Ambient Conditions

AFM measurements are routinely performed at ambient conditions and we might undermine the fact that some dynamic processes proceed in this environment. The illustrative example is taken from studies of fluoroalkanes – $F(CF_2)_n(CH_2)_mH$ - F_nH_m-, which are molecules that form different self-assemblies due to dissimilar nature of their hydrogenated and fluorinated parts [1]. When a solution containing $F_{12}H_{20}$ and $F_{12}H_8$ molecules was spread on mica substrate, self-assemblies of two types were formed on the substrate. The topography and surface potential images, which were recorded in single-pass Kevin force microscopy (KFM), in Figure 2A revealed the compact domains and arrays of spirals. The spirals arrays are slightly higher than the compact domains but their surface potential are practically identical. The images were recorded within the 1st hour after the preparation and 3 hours later the compact domains vanished from the surface as seen from the images in Figure 2B. The arrays of
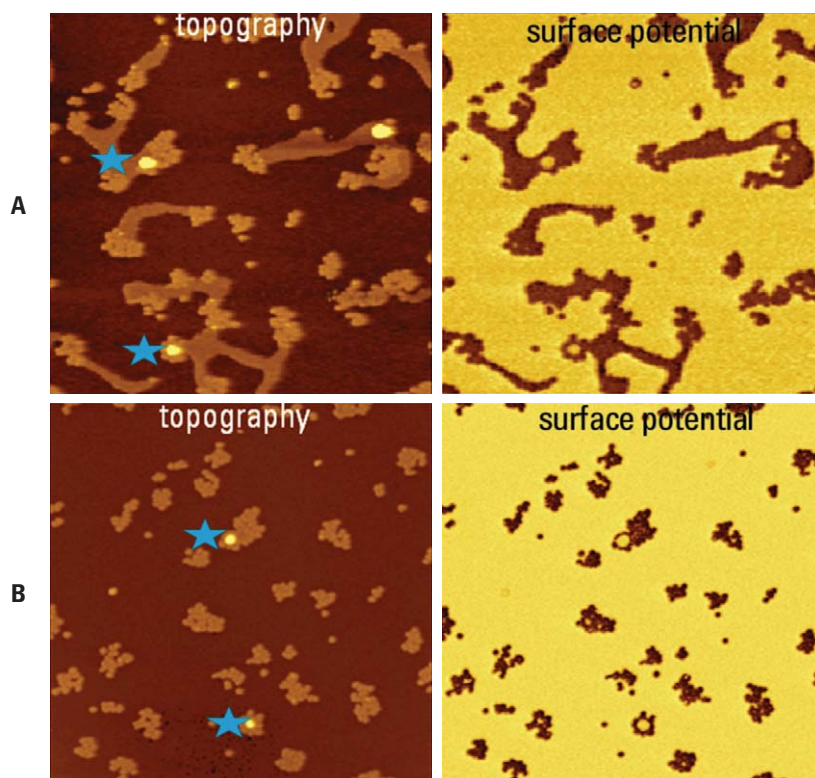

Figure 2. (A) AFM images of $F_{12}H_{20}$ and $F_{12}H_8$ self-assemblies on Si substrate. The sample was examined within 1 hour after its preparation. (B) AFM images of the same sample location 3 hours later. The images were recorded at ambient conditions. The contrast covers height corrugations in the 0-9 nm range, surface potential variations in 0-1.64 V range. Scan size: 3 µm.

on graphite and MoS$_2$ are shown in Figure 3. These structures are characterized by the spacings of 1.6 nm and 3.2 nm that are consistent with the extended single and double length of these molecules. Therefore the observed patterns are most likely associated with chains structure of dodecanol lamellae similar to those visualized in STM images of dodecanol on graphite [4]. Traces of molecular structures with similar and larger spacings, which can be found in AFM images on graphite, might be caused by volatile molecules of fragrance components and short chained alkanes.
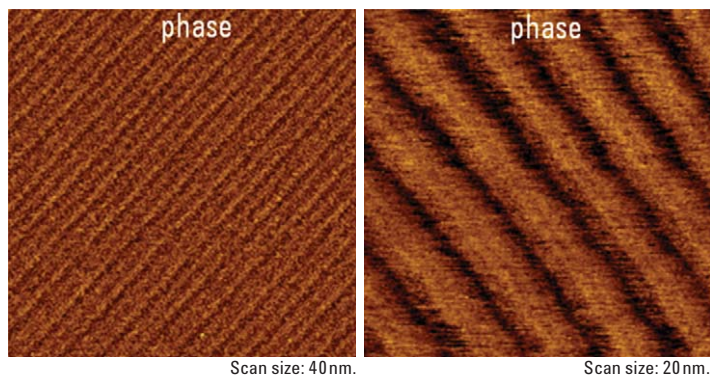

Scan size: 40 nm.   Scan size: 20 nm.

Figure 3. AFM images of dodecanol layer on graphite and MoS$_2$ substrates. The contrast covers the phase variations in the 0-10 degrees range.

Examples of AFM Applications in Different Environments

Observations of single macromolecules are one of the attractive AFM applications that start with visualization of DNA molecules. First synthetic macromolecules, which were portrayed with AFM, were single strands of block copolymer of polymethylmethacrylate (PMMA) and polystyrene (PS) [5]. The single macromolecules of the block copolymer were transferred from a water sub-phase of a Langmuir trough onto a mica substrate. The AFM images showed that hydrophilic PMMA segments were unfolded and the hydrophobic PS segments were coiled. On a change of humidity from moderate to 95% RH (RH-relative humidity) a reversible coiling of PMMA segments were monitored with the AFM. Similar structural reorganization was monitored for individual macromolecules of star-polymer, which was prepared from poly(n-butyl methacrylate) (PBMA) and poly(ethylene glycol) methyl ether methacrylate (PEGMA) using multifunctional macroinitiator. PBMA is forming the core of the polymer and PEGMA hydrophilic arms are extended away on mica substrate [6]. This conformation is clearly seen in AFM images recorded at low and moderate humidity, Figure 4A. At conditions of high humidity the molecules are changing their conformation to globular that is reflected in their height increase,
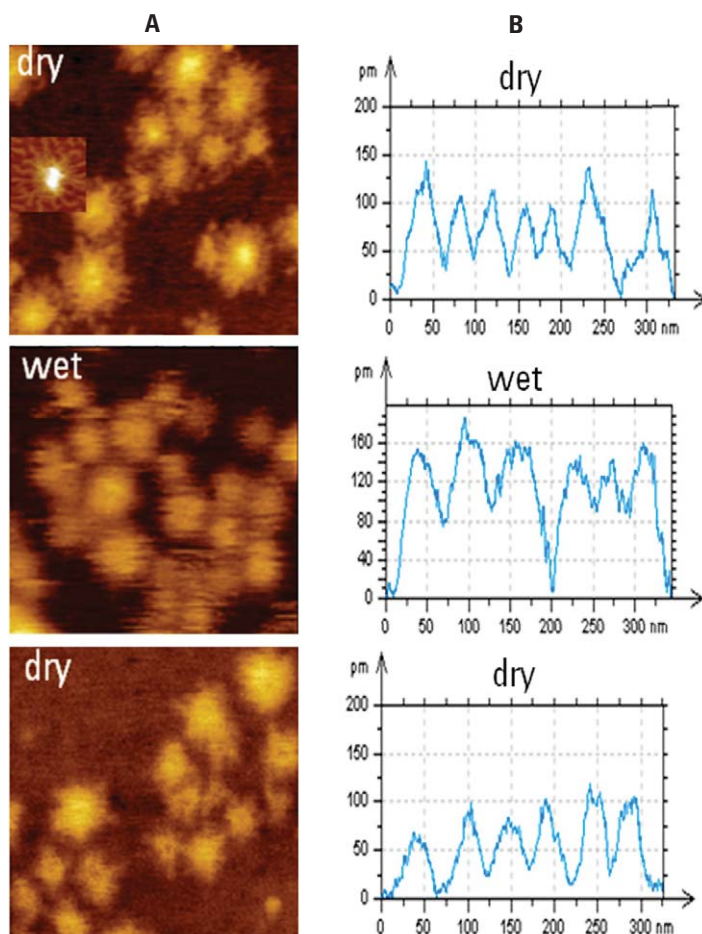

Figure 4. (Left) Topography images of star-shaped block copolymer on mica substrate in dry and wet (95%RH) environment. A high-resolution pattern of the macromolecule is inserted in top image. (Right) Topography cross-section profiles taken across of several macromolecules. Scan size: 250 nm.

Figure 4B. This can be tentatively explained by an aggregation of molecular arms with water molecules. This process is reversible and the initial conformation was restored when the sample was dried.
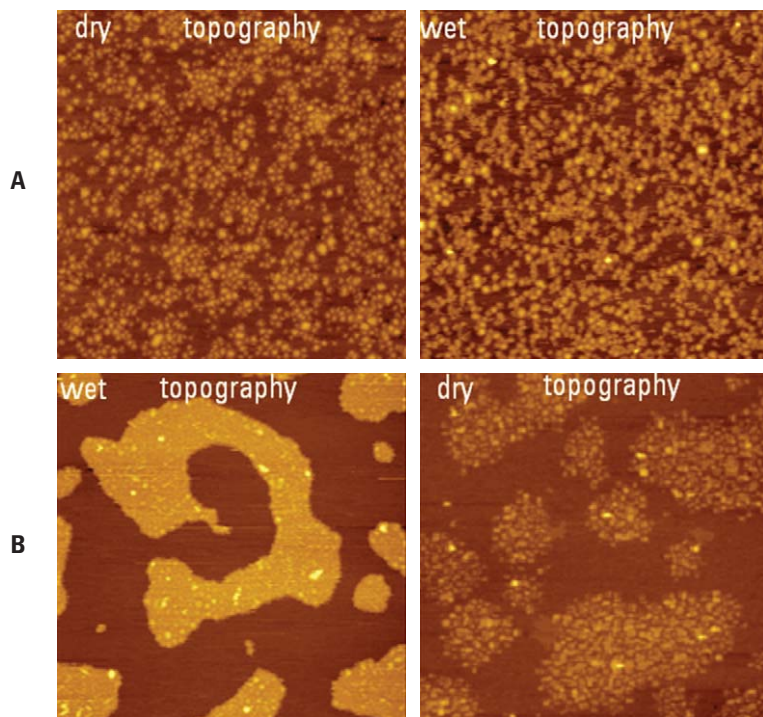
Figure 5. AFM images of star-shaped block copolymer on mica substrate in dry and wet (95%RH) environment. The contrast covers height corrugations in the 0-0.8 nm range. Scan size: 2 μm.

On the larger scale the humidity-induced transformations were first less noticeable with only through height changes of individual molecules, Figure 5A. However after several hours in wet environment the individual molecules formed the compact domains most likely through intermolecular interactions of peripheral hydrophilic segments, Figure 5B. The results of drying the conformational changes led to a "decomposition" of the domains into individual molecules which adopt the conformation with the stretched hydrophilic arms. The demonstrated monitoring of structural molecular changes caused by humidity changes can be substantially broaden to other molecular systems. A presence of ultrathin water layer on mica surface in humid atmosphere can promote different self-assembled processes such as described in [7], where the *ex-situ* AFM monitoring has been applied for visualization of the water-induced peptide self-organization.

Fluoroalkanes, F_nH_m, form different self-assembled structures such as spirals, toroids, ribbons and their intermediates. An energy balance in these self-assemblies is quite delicate and transformations of one type of self-assembly to another can be promoted by various stimuli including organic vapors [2]. It was shown that an exposure of $F_{14}H_{20}$ adsorbate, which was prepared by spin-casting from decalin solution on mica, to hexafluoroxylene (HFX) vapor initiated a conversion of the straight ribbons to bent ribbons and spirals. In the experiments with a HFX born sample, a decalin vapor triggered a transformation of the spirals to straight ribbons. The conversion of the spirals to toroids was also observed when the $F_{14}H_{20}$ sample on Si wafer spent 2 days in humid atmosphere [3]. Recently we have extended the experiments in humidity to methanol and dodecanol environments. In these studies we used single-pass KFM in the intermittent contact that avoids screening of local electric properties common for non-contact KFM applications [8].

$F_{14}H_{20}$ spirals are commonly seen in the fluroalkanes adsorbate on Si substrate, which are prepared by spin-casting of their solutions in perfluorodecalin. Topography images in Figures 6A-B reveal the arrays of spirals, which are between 3 and 4 nm in height. In between the arrays a thin layer of fluoroalkane molecules covers the substrate. According to KFM data [3] these molecules are lying flat so that their dipole moment doesn't contribute to surface potential the way the vertically oriented molecules of the self-assemblies do. When the sample environment was changed to

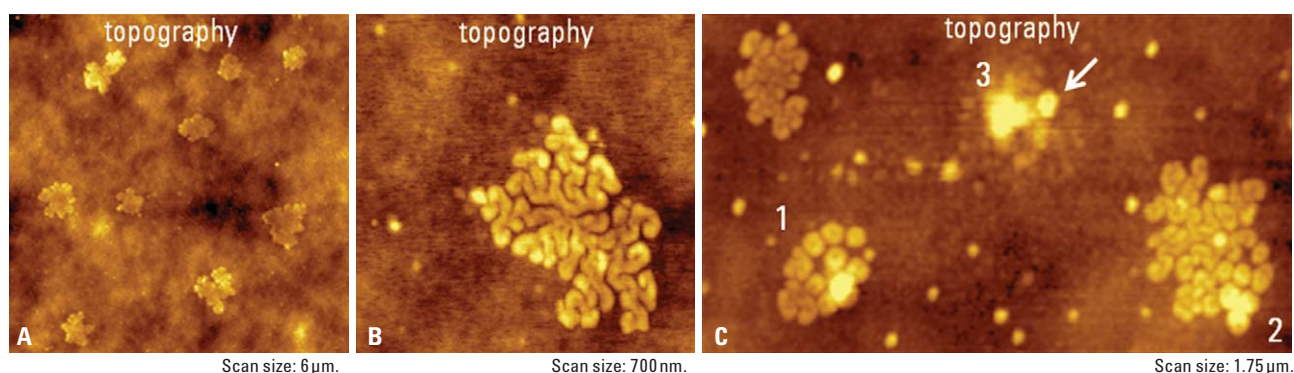Scan size: 6 μm. Scan size: 700 nm. Scan size: 1.75 μm.

Figure 6. AFM images of $F_{14}H_{20}$ self-assemblies on Si substrate in dry (A, B) and in 95%RH (C) environments. In C a white arrow indicates a single toroid self-assembly and numbers 1-3 designated the arrays and location that underwent structural changes. The contrast covers height corrugations in the 0-8 nm range in A, in the 0-6 nm range in B and in the 0-12 nm range in C.
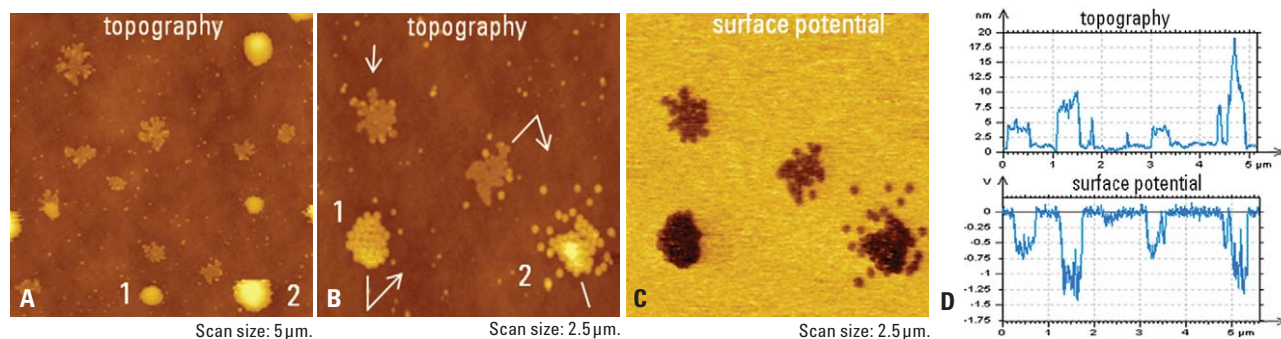
Figure 7. (A-C) AFM images of $F_{14}H_{20}$ self-assemblies on Si substrate in environment of dodecanol vapor. (D) Cross-section profiles taken in topography (B) and surface potential (C) images across the direction indicated in B with white lines and arrows. The contrast covers the height corrugations in the 0-60 nm range in A, in the 0-20 nm range in B and the potential variations in the 0-2.2 V range in C.

humid with 92-95% RH and it stayed there for many hours, several effects were noticed. First of all, one can see a formation of nanodroplets of condensed water in different sample locations some of them are the arrays of $F_{14}H_{20}$ spirals. If additional amount of water was not injected into the chamber the droplets slowly evaporated leaving toroids structures at their formed locations in the spirals arrays. Two such locations (#1 and #2) are marked in the topography image in Figure 6C. Newly formed toroids are more bulky than nearby spirals whereas the latter are also slightly increased in height compared to their dimensions in air. This observation hints on a formation of water-fluoroalkane aggregate that facilitate the spirals-toroid conversion. Additionally one can also see the surface locations free of the $F_{14}H_{20}$ spirals where water droplets have been present. One of such locations is marked as #3 in Figure 6C. It is likely that a water nanodroplet has perturbed this area making it elevated and structured into small grains with one bulky toroid emerged.

Similar changes of spirals' dimensions and their slow transformation into toroids was observed in methanol vapor [9]. The images in Figure 7A-C demonstrate the effect of dodecanol vapor. Several bright patterns in topography image (Figure 7A) represent dodecanol droplets condensed on the arrays of $F_{14}H_{20}$ spirals. This process was promoted by a slight cooling of the sample environment, 5-8 degrees below room temperature. On return to room temperature, these droplets evaporated

and left a set of toroids instead of spirals as seen from a comparison of locations #1 and #2 in Figures 7A-B. At the location #2 a number of toroids were spread away most likely in presence of the dodecanol droplet that covered them. The comparison of the arrays of spirals and sets of newly formed toroids in topography and surfaces potential images (Figures 7B-C) showed that these structures are quite different. These differences are best seen in the cross-section profiles (Figure 7D), which were taken along the "zigzag" direction marked with white arrows and lines in the topography image. The cross-section profiles have revealed that the toroids are much higher and exhibit stronger negative potential. The effects are most likely related to a presence of dodecanol molecules in the toroids or closely attached to them. This suggestion was supported by the fact that after opening the chamber to air these differences were practically eliminated. In case of the toroids formed in presence of water (Figure 6C), the height increase was similar but the changes of surface potential much smaller. They also disappeared after the sample was brought to ambient conditions (humidity ~40% RH). These observations indicate that electrostatic interactions between the fluoroalkane and polar water and alcohol molecules are involved in the self-assembly process of $F_{14}H_{20}$. High surface potential (~-1.25V) in the suggested complexes of dodecanol molecules and the fluoroalkane self-assembly requires a better understanding.

Compositional AFM imaging of block copolymers is one of the common applications of this technique in studies of polymer materials. A dissimilar nature of the polymer blocks in these materials leads to microphase separation with typical spacings in the 5-100 nm range. When block copolymer films are prepared on flat substrates by spin-casting of their solution the equilibrium morphology might not be formed during fast evaporation of the solvent. In such cases thermal annealing of the block copolymer films well above their glass transition temperatures (T_g) is applied to achieve the regular microphase separated patterns. The latter depends on the nature and volume of the components and can be properly chosen to address the needs of nanoscale lithography and design of nanoporous structures. AFM has been applied for *ex situ* and *in situ* monitoring of thermal annealing of block copolymers and visualization of dynamics of structural defects [10]. Swelling of block copolymer films in vapor of common solvent, which initiate molecular motions of the components, is alternative procedure for achieving equilibrium microphase morphology of block copolymers [11]. In this way there is no danger of heating-related problems of unwanted polymer oxidation. An example of AFM *in situ* observations of a solvent-vapor assisted annealing of triblock copolymer poly(styrene)-*b*-poly(butadiene)-*b*-poly(styrene) (PS-*b*-PB-*b*-PS) film on Si substrate is shown in Figures 8A-D. As PS is the major component in the examined polymer its morphology is characterized by PB cylinders imbedded into PS matrix. In
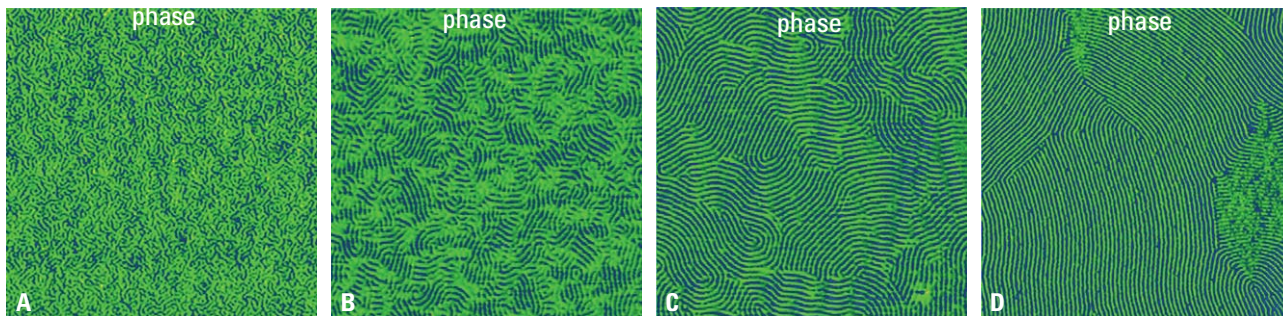
Figure 8. AFM images of thin film of triblock copolymer PS-*b*-PB-*b*-PS on Si substrate. The image in A was obtained immediately after toluene was injected into the environmental chamber. The images in B-D were recorded after 3 hours intervals. The contrast covers the phase changes in the 0-20 degrees range. Scan size: 2.5 µm.

the spin-cast film the PB cylinders are short and curved (Figure 8A) and the microstructure exhibits no long-range order. The situation gradually changed with the film exposure to toluene vapor. The in-plane cylinders become extended and formed the ordered domains of hundreds of nanometers in size at 3 hours exposure. On further vapor-induced annealing the extended cylinders and their domains reached several microns in size, Figures 8C-D.

In the attempt to use the poly(ethylene oxide−*b*-methyl methacrylate-*b*-styrene) (PEO-*b*-PMMA-*b*-PS) morphology as a nanoporous media thin films of this block copolymer were annealed in benzene vapor at different humidity [12]. This motivation was based on the high lateral order and facile degradability of the constituents of this block copolymer. In ideal nanoporous morphology the vertically oriented PMMA cylinders should be perfectly ordered (and finally etched away) within the PS matrix with PEO blocks interfacing these components. The initial 20-nm thin film was prepared on a Si substrate by spin-casting its benzene solution. The morphology changes that accompanied the annealing of ultrathin film of this block copolymer in benzene vapor at moderate humidity of 40%RH are illustrated in Figures 9A-B. The images in Figure 9A show the gradual surface changes after the injection of benzene. The left image was recorded in the scanning up direction and the initial benzene effect caused the disappearance of small bright domains inside the surface depressions. The effect can be explained by dissolving of minor blocks. In the continuing images (middle and right) the surface order was gradually changing and

nanoscale features become smeared. This observation is consistent with the fact that benzene is a good solvent for this block copolymer. The morphology changes were stopped by opening the chamber to air and the sample morphology was slightly changed as compared with the initial one (left image in Figure 9B). Further morphology changes, which finally led to the microphase separation pattern with in-plane cylinders [13], are presented in the middle and right images of Figure 9B. In another experiment the PEO-*b*-PMMA-*b*-PS film was deposited from its benzene solution on oriented polytetrafluoroethylene (PTFE) layer, which was prepared by a unidirectional rubbing of this polymer on glass at 300°C. In this case the vapor-induced annealing lead to the well-oriented structure with two preferential orientations of cylinders: along the rubbing direction and perpendicular to

it, Figure 10. This example emphasizes the role of the substrate in defining the morphology of block copolymers in thin layers.

A combined use of environmental studies with compositional imaging of heterogeneous polymers can make easy recognition of the individual components. Selective swelling induces a lowering of T_g of a particular constituent that provokes a change of its local mechanical and electric properties and the related image contrast. For example an increase of humidity induces a swelling of water channels in Nafion membranes and the latter became pronounced in phase images and in surface potential images. Similar, the high-humidity swelling of hydrophilic poly(styrene sulfonate)(PSS) domains lowered their surface potential, and this component became clearly distinguished in surface potential
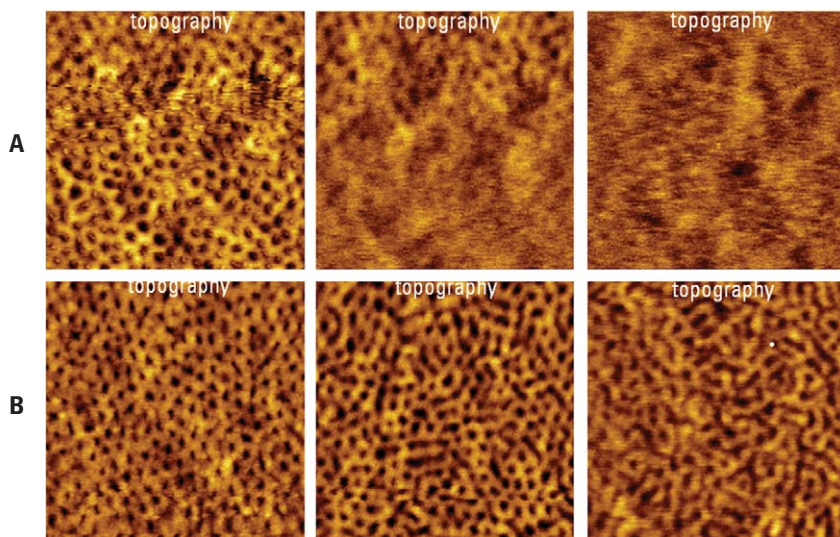

Figure 9. AFM images of ultrathin film of PEO-*b*-PMMA-*b*-PS triblock copolymer on Si substrate. The images in A were recorded in benzene vapor. The images in B were recorded in air. The contrast covers the height corrugations in the 0-4 nm range. Scan size: 700 nm.

6

images of PEDOT:PSS blend, (PEDOT - poly(3,4-ethylenedioxythiophene), which is the important component of organic solar cells and transistors. These examples were described in the previous Application Note [13]. Here we present the combined use of environmental imaging and detection of electrostatic force gradient (dC/dZ), which provides the information about local dielectric properties of materials [14, 15]. In single-pass measurements of topography, surface potential and dC/dZ the electrostatic force interactions are measured at low frequency (ω_{elec} = 3-5 kHz) whereas tracking of topography is arranged at the resonant frequency of AFM probes (typically in the 50-350 kHz range). The electrostatic force in stimulated by applying AC voltage at ω_{elec} and its response at and $2\omega_{elec}$ is employed, respectively, for surface potential and dC/dZ studies. The polymer blend consisting of equal amounts of PS and poly(vinyl acetate) was examined with dC/dZ measurements at various humidity and in methanol and toluene vapors.

Topography and dC/dZ images (amplitude and phase), which are presented in Figures 11A-C, were collected in the scan direction from bottom to top. At the beginning of the scan 2 ml of methanol were injected into the chamber and the methanol vapor effect becomes noticeable at the middle of the scan. Initial morphology of PS-PVAC blend is characterized by the micron-size spherical domains embedded into a matrix, Figure 11A. In recent study of PS-PVAC in UHV [16] the dielectric contrast of the domains has changed at temperatures near T_g of PVAC and, therefore, the domains were
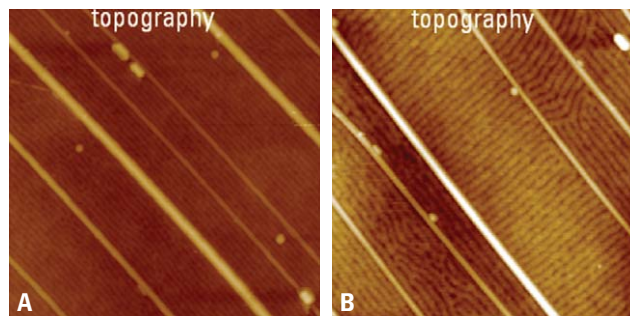

Figure 10. AFM images of thin film of PEO-*b*-PMMA-*b*-PS triblock copolymer on rubbed PTFE layer. The contrast covers the height corrugations in the 0-10 nm scale. Scan size: 3 µm.

assigned to this component. A bright appearance of the spheres in the dC/dZ amplitude image in Figure 11B is consistent with the assignment. There was practically no contrast in the dC/dZ phase image when imaging was performed in air, Figure 11C. The image changes induced by methanol vapor become noticeable in all three images. In the topography image narrow rims, which surround the spheres and reflect an immiscibility of the blend components, disappeared due to swelling and expansion of the PVAC domains. On methanol exposure the dC/dZ amplitude signal has substantially increased. The dC/dZ phase contrast most likely reflects complex permittivity of PVAC in swollen state at a particular frequency. These changes were reversible and immediately disappeared as the chamber was opened to air.

Concluding Remarks

This application note is written to bring the attention of AFM practitioners to capabilities of environmental studies, which are not fully developed and appreciated but which offer unique possibilities for characterization of different materials. A collection of practical examples discussed above demonstrates the strength of AFM studies in different gas environments for organic and polymer samples. The solvent and water molecules initiate swelling and structural transformations in a number of samples that helps identification of the components of multi-component materials and explore novel phenomena at the nanoscale level. A combined use of environmental imaging and AFM-based methods of high-resolution visualization of surface structures and local mechanical and electric studies is the solid basis for comprehensive nanoscale characterization of materials.
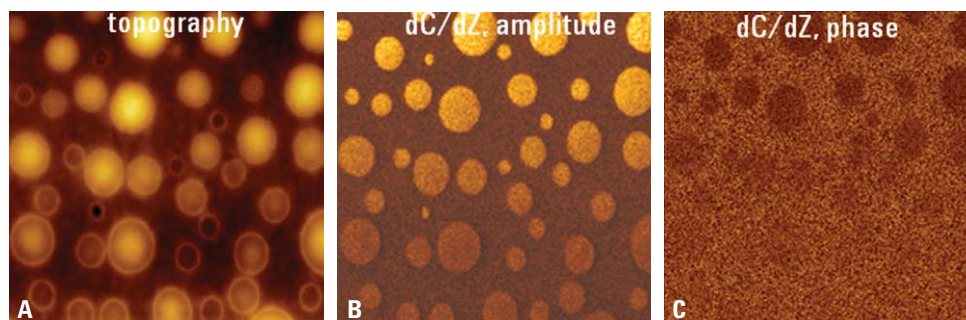
Acknowledgments

Figure 11. AFM images of 80-nm thick film of PVAC/PS blend on ITO glass. The images were obtained by scanning from bottom to top. The methanol was injected at the beginning of the scan (scan rate 0.8 Hz). The contrast covers height corrugations in the 0-35 nm range, dC/dZ amplitude alternations in the 0-180 mV range and dC/dZ phase changes in the 0-20 degrees range. Scan size: 3 µm.

References

1. J.F. Rabolt, T.P. Russell, and R.J. Twieg "Structural studies of semifluorinated n-alkanes. 1. Synthesis and characterization of $F(CF_2)_n(CH_2)_mH$ in the solid state" *Macromolecules* **1984**, *17*, 2786–2794.

2. A. Mourran, B. Tartsch, M. Gallyamov, S. Magonov, D. Lambreva, B.I. Ostrovskii, I.P. Dolbnya, W.H. de Jeu, and M. Moeller "Self-assembly of the perfluoroalkyl-alkane F14H20 in ultrathin films" *Langmuir* **2005**, *21*, 2308–2316.

3. J. Alexander, S. Magonov and M. Moeller "Topography and surface potential in Kelvin force microscopy of perfluoroalkyl alkanes self-assemblies" *J. Vac. Sci. Techn. B,* **2009**, *27*, 903–911.

4. C.L. Claypool, F. Faglioni, W.A. Goddard III, H.B. Gray, N.S. Lewis, and R.A. Marcus "Source of image contrast in STM images of functionalized alkanes on graphite: a systematic functional group approach" *J. Phys. Chem. B* **1997**, *101*, 5978–5995.

5. J. Kumaki, Y. Nichikawa, and T. Hashimoto "Visualization of Single-Chain Conformations of a Synthetic Polymer with Atomic Force Microscopy" *JACS* **1996**, *118*, 3321–3322.

6. G. Kreutzer, C. Ternat, T.Q. Nguyen, C.J.G. Plummer, J.-A. E. Månson, V. Castelletto, I.W. Hamley, F. Sun, S.S. Sheiko, and H.-A. Klok "Water-soluble, unimolecular containers based on amphiphilic multiarm star block copolymers" *Macromolecules* **2006**, *39*, 4507–4516.

7. H. Li, F. Zhang, Y. Zhang, M. Ye, B. Zhou, Y.-Z. Tang, H.-J. Yang, M.-Y. Xie, S.-F. Chen, J.-H. He, H.-Pi. Fang and J. Hu "Peptide Diffusion and Self-Assembly in Ambient Water Nanofilm on Mica Surface" *J. Phys. Chem. B,* **2009**, *113*, 8795–8799.

8. H. Sugimura, Y. Ishida, K. Hayashi, O. Takai, N. Nakagiri "Potential shielding by the surface water layer in Kelvin probe force microscopy" *Appl. Phys. Lett.* **2002**, *80*, 1459–1461.

9. S. Magonov and J. Alexander "Single-Pass Kelvin Force Microscopy and dC/dZ Measurements in the Intermittent Contact: Applications to Polymer Materials" *Beilstein Journ. Nanotech.* **2010**, submitted.

10. C. Harrison, D.H. Adamson, Z. Cheng, J.M. Sebastian, S. Sethuraman, D.A. Huse, R.A. Register, P.M. Chaikin, "Mechanisms of ordering in striped patterns" *Science* **2000**, *290*, 1558–1560.

11. G. Kim and M. Libera "Morphological Development in Solvent-Cast Polystyrene–Polybutadiene–Polystyrene (SBS) Triblock Copolymer Thin Films" *Macromolecules*, **1998**, *31*, 2569–2577.

12. J. Bang, S.H. Kim, E. Drockenmuller, M.J. Misner, T.P. Russell and C.J. Hawker "Defect-free nanoporous thin films from ABM triblock copolymers" *JACS* **2006**, *128*, 7622–7629

13. J. Bang, B.J. Kim, G.E. Stein, T.P. Russell, X. Li, J. Wang, E.J. Kramer and C.J. Hawker "Effect of Humidity on the Ordering of PEO-based Copolymer Thin Films", *Macromolecules* **2007**, *40*, 7019–7025.

14. S. Magonov, and J. Alexander "Compositional mapping of materials with single-pass Kelvin force microscopy" Application note EN 5900-0000; Agilent Technologies, Inc. March 4, **2010**.

15. L. Fumagalli, G. Gramse, D. Esteban-Ferrer, M.A. Edwards, and G. Gomilla, "Quantifying the dielectric constant of thick insulators using electrostatic force microscopy" *Appl. Phys. Lett.* **2010**, *96*, 183107–183109.

16. C. Riedel, R. Sweeney, N.E. Israeloff, R. Arinero, G.A. Schwartz, A. Alegria, Ph. Tordjeman and J. Colmenero, "Imaging dielectric relaxation in nanostructured polymers by frequency modulation electrostatic force microscopy" *Appl. Phys. Lett.* **2010**, *96*, 213110–213112.

AFM Instrumentation from Agilent Technologies

Agilent Technologies offers high-precision, modular AFM solutions for research, industry, and education. Exceptional worldwide support is provided by experienced application scientists and technical service personnel. Agilent's leading-edge R&D laboratories are dedicated to the timely introduction and optimization of innovative and easy-to-use AFM technologies.

www.agilent.com/find/afm

Americas

Canada	(877) 894 4414
Latin America	305 269 7500
United States	(800) 829 4444

Asia Pacific

Australia	1 800 629 485
China	800 810 0189
Hong Kong	800 938 693
India	1 800 112 929
Japan	0120 (421) 345
Korea	080 769 0800
Malaysia	1 800 888 848
Singapore	1 800 375 8100
Taiwan	0800 047 866
Thailand	1 800 226 008

Europe & Middle East

Austria	43 (0) 1 360 277 1571
Belgium	32 (0) 2 404 93 40
Denmark	45 70 13 15 15
Finland	358 (0) 10 855 2100
France	0825 010 700*
	*0.125 €/minute
Germany	49 (0) 7031 464 6333
Ireland	1890 924 204
Israel	972-3-9288-504/544
Italy	39 02 92 60 8484
Netherlands	31 (0) 20 547 2111
Spain	34 (91) 631 3300
Sweden	0200-88 22 55
Switzerland	0800 80 53 53
United Kingdom	44 (0) 118 9276201

Other European Countries:
www.agilent.com/find/contactus

Agilent Technologies